Hindawi
International Journal of Aerospace Engineering
Volume 2022, Article ID 7099199, 15 pages
https://doi.org/10.1155/2022/7099199

Research Article

Study of the Mechanical Properties of a CMDB Propellant Over a Wide Range of Strain Rates Using a Group Interaction Model

Kan Xie[1], **Xiaoxu Chen**[1], **Yuejie Li**[2], **Long Bai**[1], **Ningfei Wang**[1], **Yiming Zhang**[1] and **Haiyan Xiao**[3,4]

[1]*School of Aerospace Engineering, Beijing Institute of Technology, 100081 Beijing, China*
[2]*China Academy of Launch Vehicle Technology, 100076 Beijing, China*
[3]*No. 713 Institute, China Shipbuilding Industry co, Zhengzhou 450015, China*
[4]*Henan Key Laboratory of Underwater Intelligence Equipment, Zhengzhou 450015, China*

Correspondence should be addressed to Kan Xie; xiekan@bit.edu.cn

Received 29 October 2021; Revised 18 February 2022; Accepted 8 April 2022; Published 14 May 2022

Academic Editor: Angelo Cervone

Composite modified double base (CMDB) propellants are heterogeneous propellants in which properties are significantly improved by adding solid particles into the polymer matrix. A molecular group interaction model that can predict the mechanical properties of polymers through a molecular structure is used to predict the viscoelastic behavior of the CMDB propellant. Considering that the addition of solid particles will improve the crosslinking degree between polymer molecules and reduce its secondary loss peak, the input parameters of the model are modified through dynamic mechanical analysis (DMA) experimental data. By introducing the strain rate into the expression of model glass transition temperature, the mechanical properties of propellant over a wide strain range ($1.7 \times 10^{-4}\ s^{-1} \sim 3000\ s^{-1}$) are obtained. The reliability of the model is verified by comparison with uniaxial compression test data. By modifying the input parameters of the model, the effects of different mass ratios of nitrocellulose (NC)/nitroglycerin (NG) on the mechanical properties of the CMDB propellant were analyzed. The results show that the glass transition loss increases with increasing mass ratio of NC/NG, while Young's modulus and yield stress decrease.

1. Introduction

The CMDB propellant is a kind of solid propellant formed by adding high explosives and other components to improve energy characteristics on the basis of a double base propellant. It is widely used in solid rocket motors due to its unique characteristics, such as high energy density and good combustion performance [1]. Gun-launched missiles are initially driven by high-pressure gas within gun chambers to reach a muzzle speed of several hundred meters per second in a few milliseconds [2]. The propellant is compressed and deformed instantaneously; thus, the strain rate varies over a wide range of values. In high-overload applications, solid propellant particles are subjected to impact loads at a strain rate of approximately $10^2\ s^{-1}$ (the so-called intermediate strain rate) [3]. Compared with the quasistatic deformation, internal defects of the propellant develop faster in the dynamic response process under a high-overload state, and the accumulation of a large amount of damage in a short time is more likely to cause mechanical failures and reduce engine safety, leading to accidents.

However, due to the long-term lack of experimental data at intermediate strain rates, it may not be possible to verify the reliability of the existing CMDB propellant constitutive model at intermediate strain rates. In other words, there are few constitutive models that can describe the mechanical response of CMDB propellants over a wide range of strain rates, especially at moderate strain rates. Fortunately, Yang et al. [3] performed many compression experiments of the CMDB propellant at room temperature and low ($<10^2\ s^{-1}$), medium (1 to $10^2\ s^{-1}$), and high ($>102\ s^{-1}$) strain rates. According to Yang's experimental method, the CMDB

propellant was uniaxially compressed over a wide strain rate range. Therefore, the purpose of the present study is to propose a new rate-dependent model to predict the mechanical properties of CMDB propellants in various strain rate ranges. This article has made major innovations in this field to compensate for the insufficiency of the constitutive model under a moderate strain rate.

In the past 30 years, several theoretical studies have been conducted to investigate the dynamic mechanical properties of solid propellants, and remarkable results have been obtained. Siviour et al. [4] and Sunny [5] studied the dynamic mechanical properties and critical strain rate of hydroxyl-terminated polybutadiene (HTPB) over a wide range of strain rates using the split Hopkinson pressure bar (SHPB) experimental system. Combined with the dynamic mechanical analysis (DMA) experiment, Cady et al. [6] focused on the stress yield and glass transition temperature of HTPB under different strain rates. The effects of the strain rate on the yield stress and initial elastic modulus of composite modified double base (CMDB) propellants were analyzed by Chaoxiang et al. [1] and Yang et al. [3] The strain rate dependence of the ultimate stress and strain energy of CMDB propellants were revealed by Zhang et al. [7] These studies have shown that the mechanical properties of solid propellants have a strong strain rate dependence.

The establishment of a constitutive model is important for predicting the mechanical properties of a propellant and evaluating the performance of the solid rocket motor. The constitutive model established based on the phenomenological method has been widely studied because of its intuitive form and concise calculation. Ho [8] used a phenomenological nonlinear viscoelastic constitutive model that included a strain energy function to describe the deformation of the HTPB solid propellant. Sun et al. [9] and Liu et al. [10] described the deformation of solid propellants under high-strain-rate uniaxial compression using the Zhu-Wang-Tang (ZWT) model. Kunz [11] established a viscohyperelastic constitutive model describing the compression behavior of solid propellants over a wide range of strain rates based on the viscohyperelastic constitutive model proposed by Burke et al. [12]. Considering the effects of aging and damage, Yildirim and Oezupek [13] and Wang et al. [14] established thermoviscous–hyperelastic constitutive models that reflect the effects of aging on the deformation characteristics and show the damage of the high-strain-rate solid propellant under compression deformation. The macroscopic phenomenological modelling method does not consider the physical mechanism of the material and only uses appropriate mathematical expressions to describe the stress–strain behavior of the propellant based on its mechanical test data. However, as solid propellants are mixtures of polymer and solid particles, their macromechanical properties reflect their micromechanical as well as mesomechanical properties. Chen et al. [15, 16] used holes to replace dehumidified particles and established viscoelastic mesodamage models of complete and partial dehumidification of particles based on the equivalent inclusion theory. Tan et al. [17] introduced the cohesion model between particles and the matrix and established a damage model to simulate the dehumidification process of the particle interface. Tohgo et al. [18] regarded the material as a four-phase composite composed of a matrix, fully bonded particles, holes, and partially dehumidified particles and established an incremental mesodamage model. Hur et al. [19] investigated the effects of strain rate, temperature, and cyclic load to improve the constitutive model of Xu [20] by assuming that the shear modulus of the binder is a product function of the strain rate and temperature. The modelling method of mesomechanics does not involve the interactions between the various components of the matrix and those between the components of the matrix and the particles, and it cannot characterize the mechanical properties of the matrix.

An analysis of the relationship between the microstructure and mechanical properties of the propellant from a microscopic perspective can reveal the influence of the composition of the binder matrix on the mechanical properties of the propellant, help predict material properties from a microscopic perspective, clarify the mechanism of material damage, and provide a basis for the theoretical analysis of the experimental data. Based on molecular dynamics methods, Kohno et al. [21], Manaa et al. [22], and Xiao et al. [23] used a force field to describe the interaction between the molecules and atoms of each component and calculated the decomposition characteristics and mechanical properties of the single-component and two-component systems of the propellants. Because of the incomplete micromechanics theory and the limitation of computing resources, the establishment and calculation of large-scale molecular models is difficult, and the research content is limited to the microcosm. Through multiscale modelling, Porter [24] proposed a group interaction model (GIM) to predict the mechanical properties of polymers based on their molecular structure. The GIM was based on the premise that mechanical properties result from energy storage and dissipation during material deformation. By quantifying the energy storage and loss at the molecular level of the interaction between the characteristic atomic groups in the polymer, GIM enables the direct calculation of the nonlinear mechanical properties of polymers as a function of the strain, temperature, and strain rate based on their molecular structure [25]. Guan et al. [26] considered the molecular structure of natural silk, taking into account the influence of the amorphous structure on the glass transition of silk, revealing the relationship between the molecular structure of natural silk and its mechanical properties using GIM theory. Jordan et al. [27] successfully predicted the thermomechanical and engineering properties of a series of amine-cured multifunctional epoxy resins. Foreman et al. [28] predicted the mechanical behavior of three isostructural variants of HTPB and successfully predicted their impact performances. The development of the GIM yields a method for establishing the relationship between the microstructure of propellants and their macromechanical properties. However, the current research on GIMs is still focused on polymers, and there is insufficient research on propellants, especially on CMDB propellants.

This study considers the CMDB propellant commonly used in solid rocket motors and analyzes the influence of

the binder on the mechanical properties at the molecular level through GIM theory. Combining GIM theory, uniaxial compression tests, and DMA experiments, the relationship between the mechanical properties of the solid propellant and the component parameters was investigated over a wide range of strain rates. By varying the mass ratio of NC to NG in the binder, the influence of the component parameters on the mechanical properties of the propellant was analyzed. The results of this study provide a reference for the optimization design of the charge formulation over a wide range of strain rates.

2. Experiments

2.1. Uniaxial Compression Test. The composition of the CMDB propellant used in this study is given in Table 1. The particle size of HMX is 92 microns.

For the low and medium strain rate uniaxial compression tests, the GJB770B-2005 Gunpowder Test Method-Method 415.1-Compressive Strength-Compression Method was followed using a $\Phi 16 \times 20$ mm cylindrical specimen, as shown in Figure 1(a). For the high strain rate uniaxial compression tests, to reduce the radial and axial inertia effects in the small specimen [29], the length-diameter ratio was designed to be 0.5, and the specimen was a cylinder of $\Phi 10 \times 5$ mm, as shown in Figure 1(b). The propellant specimen was formed by extrusion.

The low strain rate uniaxial compression tests of solid propellants were carried out using an Instron 4505 material universal testing machine. The medium strain rate uniaxial compression tests were carried out using an Instron VHS 160/100–20 high-speed hydraulic servo testing machine. When the propellants are compressed at high speed, it may lead to the change in internal microstructure and chemical reactions under certain conditions, which may lead to combustion or explosion. When the propellant burns or explodes, it will ignite the hydraulic oil in the high-pressure oil circuit and damage the experimental equipment. According to the research of Yang et al. on medium strain rate uniaxial compression tests [3], a protection device was configured on a high-speed hydraulic servo testing machine to protect the experimental equipment. When the energetic material burns or explodes during the compression, the space formed by the protective sleeve and baffle can prevent the upward propagation of the flame and the outward splash of combustion particles. The pressure relief hole on the protective sleeve and the gap between the protective sleeve and baffle can quickly discharge the high-pressure fuel gas and reduce the pressure inside the sleeve. More details of the experimental equipment and data processing can be found in the study of Yang et al. [3]

High strain rate uniaxial compression tests of solid propellants were carried out using an SHPB.

The impact of the gas gun on the incident bar generates an incident stress pulse, which travels along the incident bar until it reaches the specimen. Part of the stress pulse reflects while the rest is transmitted through the specimen. The strain gauges placed at the incident bar and the transmission bar measure the incident strain ε_I, the reflected strain ε_R, and the transmitted wave strain ε_T.Under the assumption of one-dimensional stress wave and dynamic stress balance of the test piece, the engineering strain rate $\dot{\varepsilon}_E$, engineering stress σ_E, and engineering strain ε_E of the specimen can be calculated as follows:

Table 1: Composition of the CMDB propellant.

Composition	NC	NG	HMX	RDX	Others
Content	50%	32%	10%	/	8%

$$\begin{cases} \dot{\varepsilon}_E = -\dfrac{2C_I}{L_s}\varepsilon_R(t), \\ \varepsilon_E = -\dfrac{2C_I}{L_s}\displaystyle\int_0^t \varepsilon_R(t)dt, \\ \sigma_E = \dfrac{A_T}{A_S}E_T\varepsilon_T(t), \end{cases} \tag{1}$$

where C_I is the elastic wave velocity of the incident bar, L_S is the initial length of the specimen, A_T is the cross-sectional area of the transmission bar, A_S is the initial cross-sectional area of the specimen, and E_T is Young's modulus of the transmission bar.

Copper plate is used as pulse shaper to control the shape of incident strain pulse, and vaseline is used to lubricate the interface between compression rod and sample to reduce the radial friction between them. The schematic diagram of the experimental device for medium strain rate and high strain rate is shown in Figure 2.

The wide strain rate uniaxial compression test equipment and test conditions of the CMDB propellant are listed in Table 2. To ensure the accuracy and reliability of the test data, three parallel tests were carried out under each test condition, and the average value of the three parallel tests was taken as the final test data under this condition. All uniaxial compression tests of the CMDB propellant were carried out at room temperature (20°C).

2.2. DMA Experiments. The DMA tests measured the change in strain or stress of the polymer with time under the action of alternating stresses or alternating strains. When an external force acts on the polymer, the outside transfers mechanical energy to the polymer system. The polymer then deforms owing to its elasticity. The energy stored in the deformation is referred to as storage energy; the remainder of the energy is irreversibly dissipated and is referred to as dissipated energy [30]. The storage modulus, loss modulus, and loss tangent characteristics of the propellant are obtained through DMA experiments, which can characterize the viscoelastic properties and analyze the changes in the mechanical properties of the propellant from a molecular perspective.

The tests were carried out using a DMA-Q800 dynamic mechanical analyzer manufactured by TA Company. The size of the test piece for the DMA tests was $12.4 \times 4 \times 3.3$ mm, and the temperature range was -50–90°C (223.15–363.15 K), applied through stepwise heating

(a) Specimen for the low and medium strain rate uniaxial compression tests (b) Specimen for the high strain rate uniaxial compression tests

Figure 1: Specimen for the uniaxial compression test.

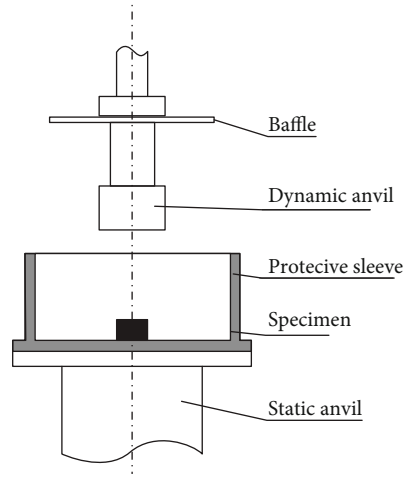

(a) Schematic of the medium strain rate uniaxial compression tests

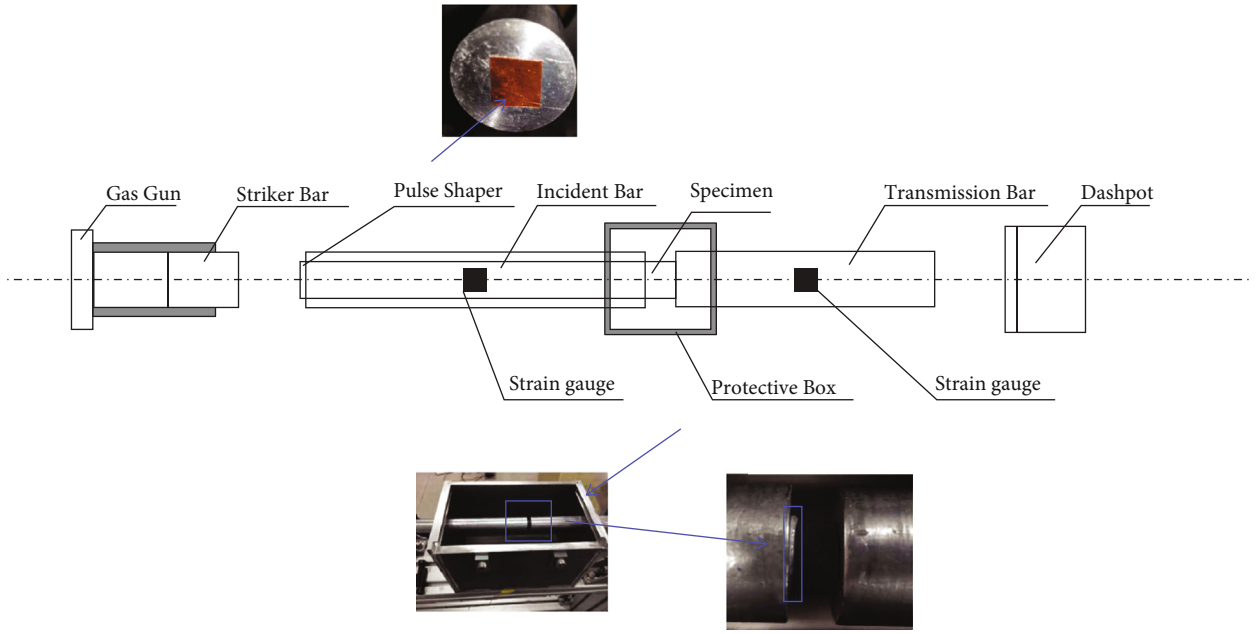

(b) Schematic of the SHPB apparatus

Figure 2: Schematic diagram of experimental device.

with a temperature step of 3°C. The specimen was supported by a single cantilever beam, the initial amplitude was 5 μm, and the loading frequency of the CMDB propellant sample was 1, 2, 5, 10, and 20 Hz.

2.3. Results and Analysis. Figure 3 shows the stress–strain curves of the CMDB propellant obtained in the uniaxial compression tests under a strain rate range of 1.7×10^{-4} s^{-1} to 3000 s^{-1} at 20°C. According to the test results, the

Table 2: Uniaxial compression test conditions.

Test type	Low strain rate	Medium strain rate	High strain rate
Equipment	Instron 4505	Instron VHS 160/100-20	SHPB
Average loading speed/launch pressure	0.2, 2, 20 (mm/min)	20, 200, 2000 (mm/s)	0.015, 0.03, 0.15 (MPa)
Engineering strain rate (s^{-1})	$1.7E-4$, $1.7E-3$, $1.7E-2$	1, 10, 100	400, 1000, 3000

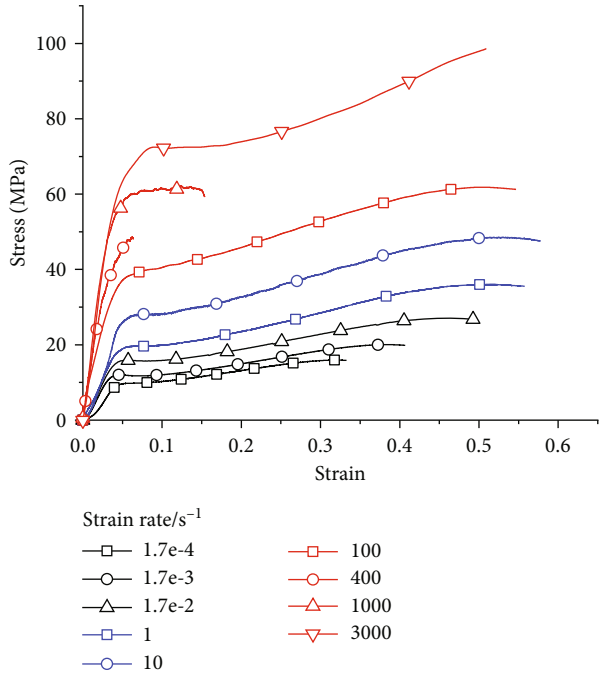

Figure 3: True stress–strain curves.

mechanical behavior of the CMDB propellant shows certain characteristics:

(1) The mechanical behavior of the CMDB propellant has an obvious strain rate dependence: the stress under constant strain increases with increasing strain rate

(2) The rate of change of the stress–strain curve for the CMDB propellant exhibits an obvious inflection point

Figure 4 shows the storage modulus, loss modulus, and loss tangent over 1–20 Hz with temperature obtained in the DMA tests. There are two inflection points in the dynamic mechanical properties of the CMDB propellant. Taking the loss tangent curve as an example, there is a small loss peak at low temperature, which corresponds to the secondary transformation (α transition) of the CMDB propellant; this is generally considered to be related to the side base movement of NC and NG. The transition peak-to-peak value of the high-temperature section is larger and corresponds to the glass transition (β transition) of the CMDB propellant, which is generally considered to be related to the main chain movement of NC and NG [31]. As the frequency increases, the α and β transition peaks of the CMDB propellant shift to higher temperatures.

3. Constitutive Model

The GIM theory was established by Porter [24] in 1995 to describe the relationship between a polymer molecular structure and its macroscopic mechanical properties. The basic assumption of GIM theory is that the mechanical properties of polymers are the direct result of energy storage and dissipation during material deformation. GIM theory quantifies the energy storage and loss at the molecular level of the interaction between characteristic groups (polymer molecular units) and converts the above assumptions into a series of continuous structure–performance relationships to construct equations of state and constitutive relationships. The GIM allows the mechanical properties related to the strain, temperature, and strain rate of polymers to be calculated directly based on the polymer molecular structure.

The CMDB propellant is a composite material composed of a binder matrix and a solid particle filler. Its mechanical properties reveal a viscoelasticity similar to that of a pure polymer, and it is also affected by solid particles and the interaction between solid particles and the binder. Based on the GIM method combined with the Mori–Tanaka mesomechanics model and considering the impact of solid particles on characteristic molecular groups, a method for predicting the mechanical properties of solid propellants based on component information is established over a wide strain rate range.

3.1. GIM Model. The geometric model of the interaction between molecular segments in GIM theory is shown in Figure 5. Each polymer segment is surrounded by six identical molecular segments. Each bendable and deformable polymer molecular segment is an inextensible cylinder with a diameter of r composed of Z characteristic group units; the length of each unit is L.

The distance between the centers of adjacent molecular segments is the same as the diameter of the segments. Adjacent molecular segments are bound by an attraction force such as the binding energy of the van der Waals force, i.e., the molecular group interaction energy, E. A potential function is introduced to describe the interaction between molecular groups. The relationship between the interaction energy and the center distance, r, of the chain segment is as follows:

$$E = E_{\text{coh}}\left[\left(\frac{r_0}{r}\right)^{12} - 2\left(\frac{r_0}{r}\right)^{6}\right]. \tag{2}$$

This can be expressed in terms of the volume ($V = L \cdot r^2$) as follows:

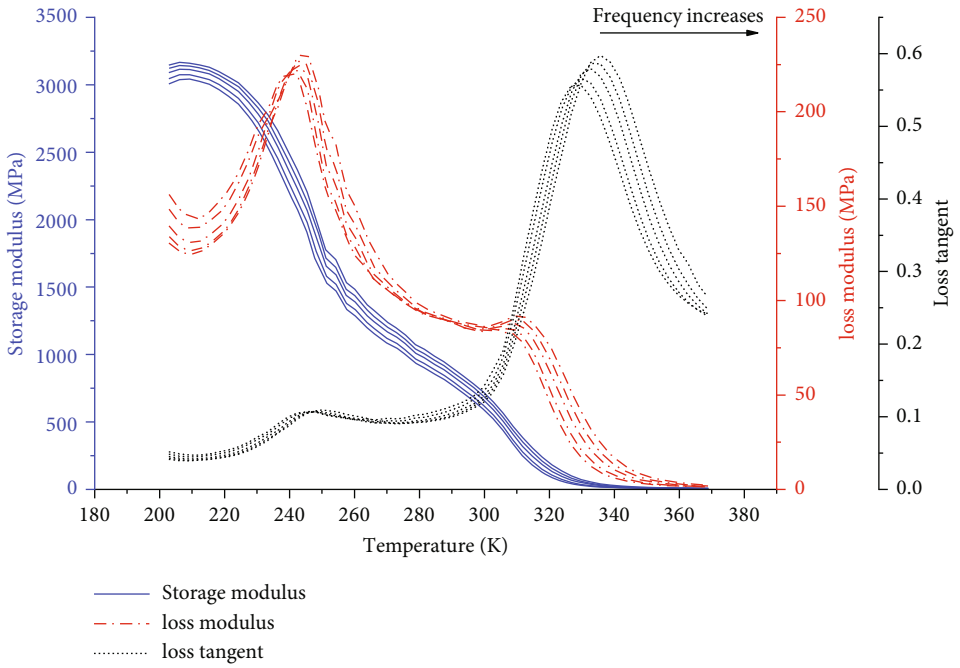

Figure 4: DMA test results.

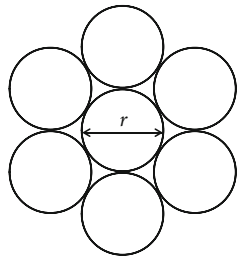

Figure 5: Interaction geometric model.

$$E = E_{\text{coh}}\left[\left(\frac{V_0}{V}\right)^6 - 2\left(\frac{V_0}{V}\right)^3\right], \tag{3}$$

where r_0 and V_0, respectively, represent the distance and volume of the center of the chain segment when a pair of molecular chain segments in contact with each other are in equilibrium at absolute zero. E_{coh} represents the value of the potential function when the distance between the centers of the chain segments is r_0, which is referred to as the zero-point binding energy.

The interaction energy, E, of molecular groups can also be expressed as $-E_{\text{coh}}$, which is the sum of the conformational energy and thermal energy:

$$E = -E_{\text{coh}} + H_c + H_T. \tag{4}$$

For crystalline and amorphous polymers, the conformational energy H_c is $0.04E_{\text{coh}}$ and $0.06E_{\text{coh}}$, respectively, which can also be summed according to the ratio of each state present. The thermal energy is obtained as follows:

$$H_T = \int_0^T \left\{ \text{NR}\frac{(6.7T/\theta_1)^2}{\left[1 + (6.7T/\theta_1)^2\right]} \right\} dT, \tag{5}$$

where θ_1 is the cooperative vibration reference temperature, N is the freedom of movement of the characteristic group, and R is the molar gas constant.

The expression for the coefficient of thermal expansion, α, is as follows:

$$\alpha = \frac{1.38C}{(E_{\text{coh}}R)}. \tag{6}$$

For most polymers at room temperature (20°C), the coefficient of thermal expansion, α, is approximately equal to the following:

$$\alpha \approx \frac{1.35N}{E_{\text{coh}}}. \tag{7}$$

The GIM has established an atomic group contribution table and selection principle for θ_1, which can determine the van der Waals volume, V_W ($V_0 = 1.26V_w$), E_{coh}, N, and θ_1 of the characteristic group based on the molecular structure of the high-reference characteristic group and the principle of atomic group addition.

In the GIM, the pressure is calculated as a function of unit volume by differentiating the potential function.

$$P = \frac{dE}{dV} = \frac{6E_{\text{coh}}\left[(V_0/V)^3 - (V_0/V)^6\right]}{V}. \tag{8}$$

The bulk modulus of the pure elastic form of the binder matrix, B_0, is the derivative of the pressure:

$$B_0 = V\frac{dP}{dV} \approx 1.7\frac{E_{\text{coh}}\left[2(V_0/V)^3 - (V_0/V)^6\right]}{\left[(V/V_0 - 1)V_W\right]}. \quad (9)$$

Considering that the addition of solid particles will affect the pure elastic bulk modulus of the propellant, the Mori–Tanaka [32] method is used to calculate the pure elastic bulk modulus, B, of the propellant.

The Mori–Tanaka expression for the pure elastic bulk modulus of particle-filled composites is

$$\begin{cases} \dfrac{B}{B_0} = 1 + \dfrac{Q}{(1 - Q\alpha_0)}, \\ Q = \displaystyle\sum_{i=1}^{n} \dfrac{c_i(B - B_0)}{[\alpha_0(B_i - B_0) + B_0]}, \\ \alpha_0 = \dfrac{3B_0}{(3B_0 + 4G_0)}, \end{cases} \quad (10)$$

where B_0 is the pure elastic bulk modulus of the matrix, G_0 is the pure elastic shear modulus of the matrix, c_i is the volume fraction of the ith solid particle, and B_i is the bulk modulus of the ith solid particle. The expression for G_0 is as follows:

$$G_0 = \frac{B_0}{\left[3/\left(1 - \tan\Delta_\beta^{1/2}\right)^2 - 0.33\right]}, \quad (11)$$

where $\tan\Delta_\beta$ is the area under the β transition peak in the loss tangent curve. Under purely elastic conditions, $\tan\Delta_\beta \approx 0$. Then, Equation (11) is substituted into the expression for α_0, resulting in $\alpha_0 = 0.67$, which will continue to be used in the subsequent calculation of the bulk modulus.

Under loading of an external force, external mechanical energy is applied to the polymer system, and part of the increased mechanical energy is stored as deformation, while the remainder is dissipated. This energy dissipation is divided into two parts: the first part is thermodynamic loss, in which energy is dissipated irreversibly in the form of heat energy; the second part is energy dissipation due to the transition of polymer states. Because polymer molecules have large molecular weights, the molecular chain is long, and the degrees of freedom are high. In addition, there is cross-linking between the molecular chains. When the molecular motion reaches a certain level, the state of the polymer will change. Under low-temperature conditions, the polymer chain is in a frozen state. When the temperature rises, the restrictions on a specific atom group are gradually lifted, the degrees of freedom in the molecule are activated, and the polymer undergoes a β transformation. However, the entire polymer chain is still constrained in a fixed position. As the temperature continues to rise, the degrees of freedom in the movement of the main chain are activated, and the polymer chain can undergo short-range diffusion movement. The degree of freedom of the movement increases from N to $1.5N$, and the substance undergoes an α transformation.

In GIM theory, the glass transition temperature, T_g, of the polymer is obtained by deriving the potential function based on the Born instability criterion. The expression for the glass transition temperature at 1 rad/s is as follows:

$$T_{gr} = 0.224\theta_1 + 0.0513\left(\frac{E_{\text{coh}}}{N}\right), \quad (12)$$

The relationship between T_g and the angular frequency, f (the angular frequency of the DMA test loading), is given by the GIM theory as follows:

$$f = f_0 \exp\left[\frac{-(1280 + 50\ln\theta_1)}{(T_g - T_{gr} + 50)}\right]. \quad (13)$$

In this equation, the reference angular frequency, f_0, is related to the Boltzmann constant, k, and Planck constant, h:

$$f_0 = \frac{k\theta_1}{h}. \quad (14)$$

Equation (13) shows that the glass transition temperature, T_g, increases roughly linearly with $\log f$. The angular frequency, f, and the strain rate, $\dot{\varepsilon}$, of the propellant have the following relationship:

$$f = \frac{\dot{\varepsilon}l_0}{2d_0}, \quad (15)$$

where l_0 is the initial thickness of the DMA test specimen and d_0 is the loading amplitude in the DMA test. The values of l_0 and d_0 in the DMA tests in this study are 3.3 mm and 5 μm, respectively.

Energy dissipation can be measured by the loss tangent (dissipated energy/energy storage). The cumulative loss tangent is defined as the total area under the loss tangent peak. GIM theory calculates the value of the cumulative loss tangent of α by quantifying the ratio of the energy dissipated due to the increase in degrees of freedom during the α transformation to the energy required for the polymer to undergo α transformation. The calculation method for the α cumulative loss tangent is

$$\tan\Delta_g \approx 0.0085\frac{E_{\text{coh}}}{N_c}, \quad (16)$$

where N_c represents the number of degrees of freedom activated when the molecular chain is stretched. The specific values are obtained from the atomic group contribution table.

The distribution of the α loss tangent, $\tan\Delta_g$, with temperature is assumed to be a Gaussian distribution function centered on the peak temperature, T_g, and divergence, s_g.

$$\tan\delta_g = \left(\frac{\tan\Delta_g}{\left(s_g\sqrt{2\pi}\right)}\right)\exp\left(\frac{-(T - T_g)^2}{2s_g^2}\right). \quad (17)$$

Compared with the glass transition loss tangent, which can be accurately quantified, the β transition is difficult to predict owing to its complexity and uncertainty. The GIM theory uses an empirical method combined with DMA tests to describe the β transition. The β transition temperature is described by the Arrhenius formula as follows:

$$T_\beta = \frac{-\Delta H_\beta}{[R \ln (f/f_0)]}, \tag{18}$$

where ΔH_β represents the activation energy of the β transformation.

The β cumulative loss tangent is also measured by the ratio of dissipated energy to stored energy during the β transition, as follows:

$$\tan \Delta_\beta \approx k_c \frac{\Delta N_\beta}{N_c}, \tag{19}$$

where ΔN_β represents the degree of freedom of the polymer that is activated by the β transformation, $\Delta N_\beta/N_c$ is the ratio of the degrees of freedom of the side group of the polymer molecule to the degrees of freedom of the main chain, and k_c is a proportional coefficient. An empirical value for k_c of 25 was obtained by analyzing a large number of polymers.

The distribution of the β transition peak is generally wider than that of the α transition peak. Similarly, the distribution of the β loss tangent, $\tan \Delta_\beta$, is described by a Gaussian function:

$$\tan \delta_\beta = \tan \Delta_\beta \frac{\exp\left[-\left(T - T_\beta\right)^2 / \left(2s_\beta^2\right)\right]}{\left(s_\beta \sqrt{2\pi}\right)}. \tag{20}$$

The expression for the distribution function of the loss tangent, tanδ, is the sum of $\tan \delta_g$ and $\tan \delta_\beta$.

According to the temperature gradient of the pure elastic bulk modulus derived above, the Young's modulus before the glass transition can be obtained as follows:

$$Y_\beta = B \exp\left[\frac{-\int_0^T \tan \delta_\beta dT}{(A \cdot B)}\right], \tag{21}$$

where the upper limit of integration, T, is the observation temperature, i.e., the ambient temperature of the propellant. The expression for A is

$$A = \frac{1.5 \times 10^5 L}{(\theta_1 \cdot M)}, \tag{22}$$

where M is the molar mass of the characteristic group.

On this basis, the expression for Young's modulus covering the range of the polymer rubber state is as follows:

$$Y_\alpha = \frac{Y_\beta}{\left(1 + \int_0^T \tan \delta_g dT\right)^2}. \tag{23}$$

The yield point is an important demarcation point for the mechanical properties of polymers, and it represents the beginning of plastic deformation. The GIM theory defines the yield point as the state point where the characteristic group units can undergo large-scale translational motion relative to each other. The mechanical yield point is equivalent to the thermal glass transition point.

The magnitude of the expansion of a unit volume from V to the glass transition state can be measured using the temperature increase and thermal expansion coefficient, α:

$$\left(\frac{\Delta V}{V}\right)_y = \alpha\left(T - T_g\right). \tag{24}$$

Substituting the expression for α into Equation (24) yields the following:

$$\left(\frac{\Delta V}{V}\right)_y = \frac{1.35\, N\left(T - T_g\right)}{E_{\text{coh}}}. \tag{25}$$

Only part of the energy input to the propellant is used to generate elastic strain, while the other part is lost through thermal dissipation or the phase change of the polymer. The strain can thus be expressed as follows, assuming that the total strain, ε, is consumed by the pure elastic strain, $\Delta V/V$, and viscous strain, ε_v:

$$\varepsilon = \frac{\Delta V}{V} + \varepsilon_v = \frac{(\Delta V/V)}{\left(1 - \tan \Delta_\beta^{1/2}\right)}, \tag{26}$$

where $\tan \Delta_\beta$ is the cumulative loss tangent of the β transition.

The yield strain can be expressed as follows:

$$\varepsilon_y(T) = \frac{1.35N\left(T - T_g\right)}{\left[\left(1 - \tan \Delta_\beta^{1/2}\right) E_{\text{coh}}\right]}. \tag{27}$$

According to the elastic modulus of the polymer before the glass transition,

$$E_e = B\left(1 - \tan \Delta_\beta^{1/2}\right)^2. \tag{28}$$

The expression for the yield stress is as follows:

$$\sigma_y(T) = \frac{1.35\, B\left(1 - \tan \Delta_\beta^{1/2}\right) N\left(T - T_g\right)}{E_{\text{coh}}}. \tag{29}$$

3.2. Input Parameters. The molecular structures of NC and NG are shown in Figure 6. The GIM input parameters of

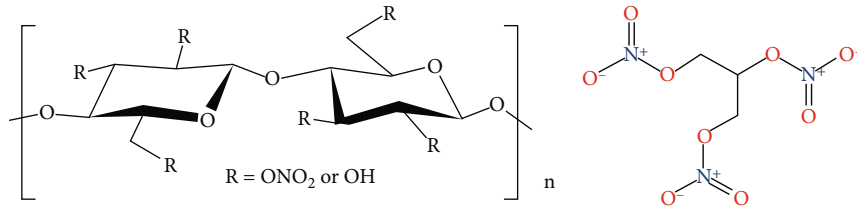

(a) Molecular structure of NC (b) Molecular structure of NG

Figure 6: Molecular structures of NG and NC.

Table 3: Input parameters of the binder.

	E_{coh} (J/mol)	N	N_c	V_w (cc/mol)	M (g/mol)
-CH-	4500	2	—	10.23	13
$-CH_2-$	4500	2	—	10.23	14
-O-	6300	2	—	5	16
-OH-	13000	2	—	8	17
$-NO_2-$	21500	4	—	14	46
NC	235070	61.3	94	337	559
NG	96900	24	12	87	227

Table 4: GIM input parameters for the CMDB propellant.

E_{coh} (J/mol)	N	N'	N_c	V_w (cc/mol)	L (Å)	ΔH_β (J)	Θ_1 (K)
150540	38.5	31.6	43.7	184.1	44.1	53065.3	364

related groups are found in the atomic group contribution table, and the GIM input parameters of the binder system are obtained based on the principle of addition. These parameters are listed in Table 3.

Unlike θ_1 and ΔN_β, the GIM input parameters E_{coh}, V_w, N, and N_c for NC and NG are obtained through addition of the values in the atomic group contribution table. The CMDB propellant binder matrix is a mixture of NC and NG. For the mixed polymer, the GIM input parameter value is calculated as a weighted average, where the weight is the fraction of the amount of substance, n_i. For example, the value of N for the binder matrix is $N_{NC} \times n_{NC} + N_{NG} \times n_{NG}$. The conversion between the mass fraction, m_i, of the ith ($i = 1, 2$) polymer and the molecular weight fraction, n_i, is calculated using Equation (30). The value of the β cumulative loss depends on the structural characteristics of the polymer molecule. For a polymer consisting of a mixture of two polymers, the β cumulative loss tangent value is expressed as Equation (31). The GIM input parameters are listed in Table 4, in which the β activation energy, ΔH_β, is obtained by fitting the β transition temperature in the 1–20 Hz DMA experiments.

$$n_i = \frac{(m_i/M_i)}{(m_{NC}/M_{NC} + m_{NG}/M_{NG})}, \tag{30}$$

$$\tan \Delta_\beta = \sum_{i=1}^{2} \tan\Delta_{\beta,i} n_i. \tag{31}$$

Table 5: Physical parameters of each component.

	Binder	RDX	HMX
Density, ρ (g·cm^{-3})	1.61	1.82	1.894
Bulk modulus, B (GPa)	/	46.43	9.4

In Equation (30), m_i represents the molar mass of the i^{th} polymer molecule.

Based on the propellant binder matrix and solid particle component parameters, the pure elastic bulk modulus is calculated. The component mass fraction is given in the propellant component information and needs to be converted into a volume fraction. The conversion relationship between the mass fraction, m_i, and volume fraction, V_i, of each component is as follows:

$$V_i = \frac{(m_i/\rho_i)}{[\sum_{i=1}^{n}(m_i/\rho_i)]}, \tag{32}$$

where V_i is the volume fraction of the ith component in the propellant, m_i is the mass fraction of the ith component, and ρ_i is the density of the ith component. The density and bulk modulus of each component in the CMDB propellant are listed in Table 5.

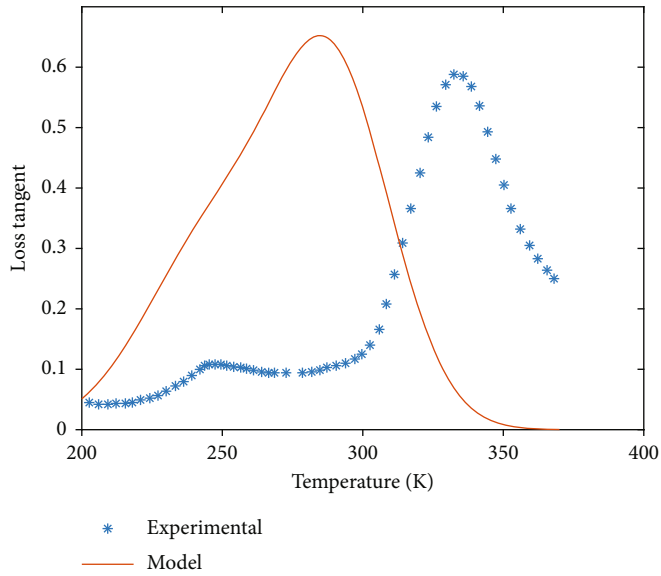

Figure 7: Prediction results for the 10 Hz loss tangent.

4. Results and Discussion

4.1. Model Verification. The mechanical loss characteristics of the propellant are predicted, and the divergence of the loss tangent distribution of α and β is determined based on DMA experiments. As shown in Figure 7, the prediction results for the loss tangent curve at 10 Hz are quite different from the experimental data. In particular, relative to the experimental data, the α transition temperature is too low, and the β transition peak is too high in the predicted results. For the glass transition temperatures predicted in the range of 1–20 Hz, the results show that the predicted α transition temperature at each frequency is relatively low.

Due to the microscopic analysis, near the surface of the solid particles, the polymer chain segments will be entangled with each other. Dehm [33] showed that solid particles are actually a function of physical cross-linking points. With increasing cross-linking point density, the free volume of the polymer decreases, the degree of restriction on the activity of the molecular chain increases, and the average chain length between adjacent cross-linking points decreases.

As the degree of cross-linking increases, the degree of freedom of movement of the polymer segment, N, will decrease. From the above assumptions, the value of N is reversed based on the experimental data. In the DMA tests, at a frequency of 10 Hz, $T_g = 334$ K. Substituting this into the expression for the glass transition temperature, the corrected value of N (N') is 31.6. When the corrected N value is used to predict the T_g values of the 1–20 Hz DMA experiments, the GIM theory can predict the glass transition temperature of the CMDB propellant well, as shown in Figure 8.

Zhou et al. [34] compared the experimental results of DMA experiments on a double base propellant and modified doublebase propellant with the same NC/NG mass ratio. The results showed that the solid particles had little effect on the value of T_β but reduced the β loss peak.

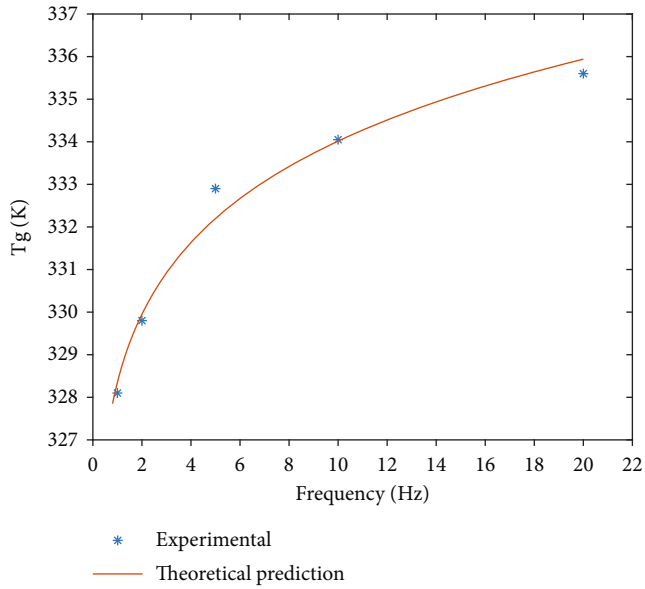

Figure 8: Glass transition temperature prediction with a corrected value of N.

In the calculation equation for $\tan \Delta_\beta$, $\Delta N_\beta / Nc$ is the ratio of skeletal degrees of freedom to degrees of freedom in the chain which is the molecular structure characteristic parameter of the polymer. It is believed that the addition of solid particles will not change this value. The proportional coefficient k_c presents the ratio of the secondary transition temperature to the peak distribution width. On the premise that k_c is a fixed value, the peak distribution width must increase as the peak temperature increases to maintain a constant total cumulative loss tangent area under the peak. It is considered that the addition of solid particles will change the width of the peak distribution resulting in changing the value of k_c.

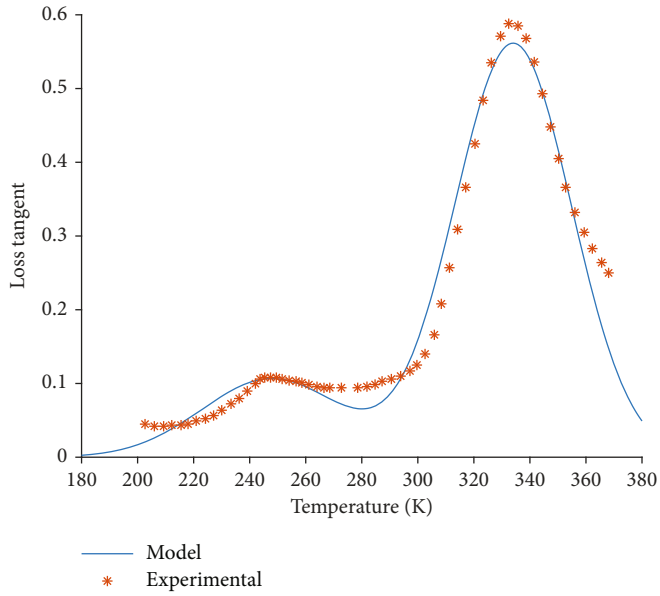

Figure 9: Prediction results for 10 Hz loss tangent with corrected values of N and k.

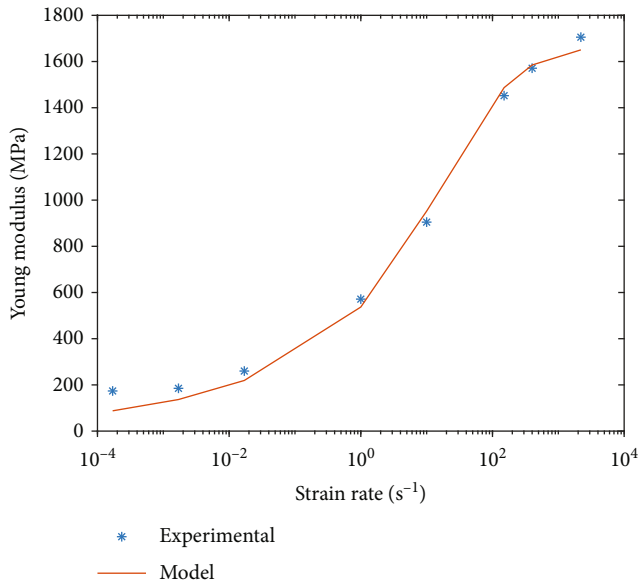

Figure 10: Young's modulus prediction.

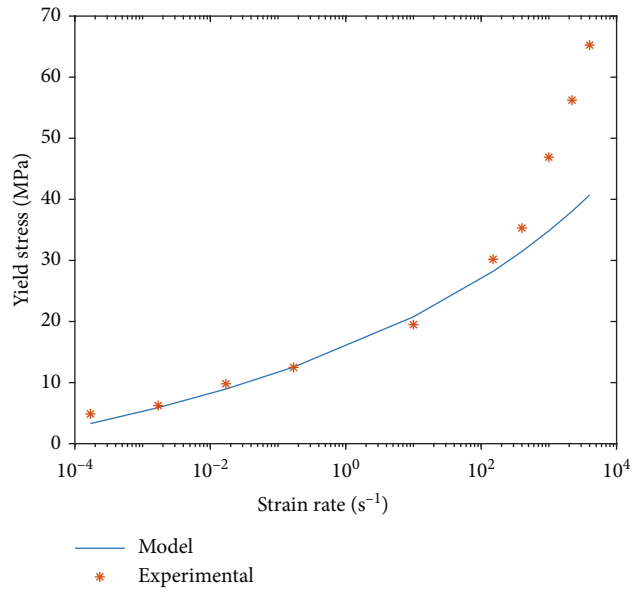

Figure 11: Yield stress prediction.

According to the DMA experimental data, the k_c value of the CMDB propellant is 8.42. By substituting the corrected N and k_c values into the loss tangent expression, the prediction of the loss tangent curve is significantly improved and is more consistent with the experimental data, as shown in Figure 9.

Young's modulus is a measure of elastic energy stored in materials, so larger energy dissipation or loss must be reflected in lower Young's modulus [35]. Bondi [36] pointed out that if the mechanism of mechanical energy conversion to heat can be identified, the empirical proportional relationship between the loss tangent and elastic modulus temperature gradient can be used to predict the elastic modulus. Equation (21) is given on this basis. When the temperature is higher than the glass transition temperature, this simple proportionality fails, so a separate relationship needs to be called to cover the glass transition temperature and above. Equation (23) is taken from the original GIM model [24] to predict Young's modulus at and above the glass transition temperature because the glass transition has a very high energy dissipation factor (loss tangent).

Based on the input values of the pure elastic bulk modulus and loss tangent of the CMDB propellant, compressed Young's modulus could be calculated over a wide strain rate range using the aforementioned GIM prediction method. Comparing the results with the experimental data, it can be seen that this prediction method is accurate and reliable. The prediction results are shown in Figure 10. The temperature and strain rate dependence of Young's modulus can be

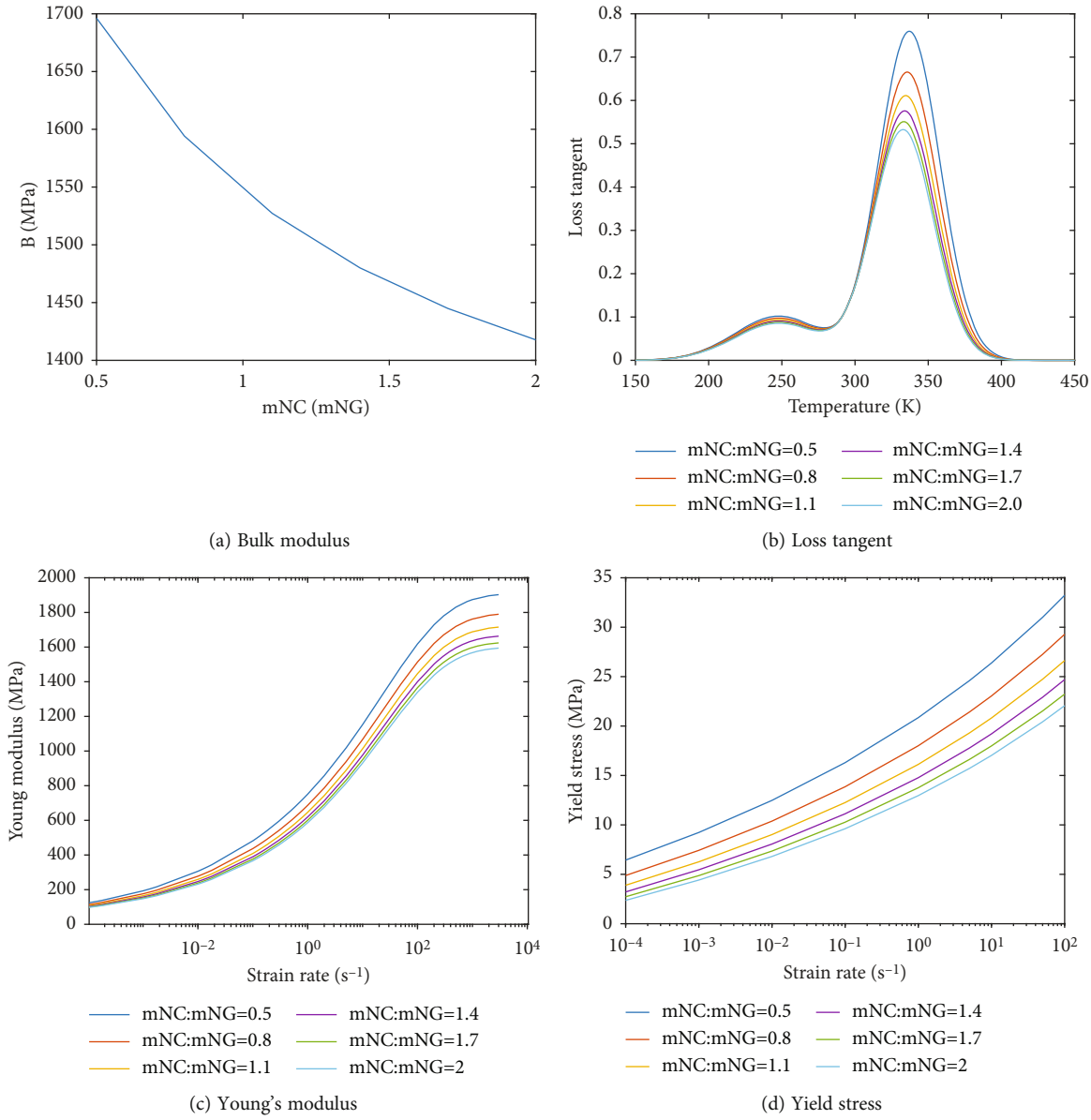

Figure 12: Mechanical properties of the propellant with different NC/NG mass ratios.

attributed to the strain rate dependence of the glass transition temperature and secondary transition temperature. Under the condition of small strain, the value of compressive Young's modulus is the same as that of tensile Young's modulus.

Similarly, the yield stress can be predicted based on the data in Table 4. The prediction results are shown in Figure 11. Comparing the prediction results with the experimental data shows that the GIM method is very effective for predicting the yield stress of the CMDB propellant in the low and medium strain rate ranges. However, the prediction of the yield stress in the high strain rate range is poor.

It can be seen from the expression for the yield stress in the GIM model that at a certain temperature, the growth of the yield stress is approximately linear with the logarithm of the strain rate. In fact, when the strain rate reaches a certain value, there is an inflection point in the change in the yield stress with the strain rate, resulting in a significant increase in the yield stress growth rate at high strain rates. Yang et al. [3] used DMA experiments on a CMDB propellant and the detachment-shift-reconstruction (DSR) analysis method to determine that the inflection point in the trends of the yield stress and other mechanical properties with the strain rate can be attributed to the change in the strain rate-related mechanism from α transformation control to a combined α and β transformation control. GIM theory indicates that the mechanical yield point is equivalent to the glass transition point in thermals, emphasizing the decisive role of the α transition without considering the effect of the β transition, and thus, it is only suitable for the prediction of yield stresses at low and medium strain rates (<100 s^{-1}).

4.2. Influence of the NC/NG Mass Ratio. Based on the content of the previous section, the mechanical properties of the propellant are predicted by varying the NC/NG mass

ratio in the propellant while keeping the other components unchanged. The changes in the mechanical properties of the propellant are analyzed as the NC/NG mass ratio is varied from 0.5 to 2.

As shown in Figure 12(a), as the mass ratio of NC to NG increases, the pure elastic bulk modulus of the propellant decreases, indicating that the ability of the propellant to resist deformation is weakened.

The influence of the NC/NG mass ratio on the tangent curve of the CMDB propellant loss is shown in Figure 12(b). The NC/NG mass ratio has little influence on the α and β transition temperatures of the propellant. When the mass ratio of NC/NG decreases, both the α and β loss peaks increase, the α and β cumulative losses also increase, and the effect of the mass ratio on the α transition is greater. These rules are consistent with the experimental results reported by Yao et al. [37]. The main reason for this phenomenon is that when the NC/NG mass ratio decreases, the free volume between molecules increases, and conformational change of the polymer chain more easily occurs, which leads to the increase of the α mechanical loss.

Young's modulus and yield stress under different mass ratios are shown in Figures 12(c) and 12(d). Yang et al.'s [3] research shows that the mechanical properties of propellants at low and medium strain rates are mainly affected by β transition, while at high strain rates, they are jointly affected by β transition and α transition. The NC/NG mass ratio has little effect on β transition but has a great influence on the α transition. Therefore, it can be seen that the mass ratio has little effect on Young's modulus and yield stress at low and medium strain rates but has a greater effect at high strain rates. With the increase in the NC/NG mass ratio, Young's modulus and yield stress of the propellant decrease.

5. Conclusion

This study utilizes GIM theory; starting from the micromolecular structure of the binder in a solid propellant, a series of physical equations are used to measure the energy storage and dissipation characteristics of the characteristic group under an external load. The influence of the discrete phase of particles is considered to establish a method for predicting the mechanical properties of solid propellants over a wide strain rate range based on their composition. When modelling the CMDB propellant, it is found that the solid particles act as physical cross-linking points, which will reduce the freedom of movement of the molecules and the cumulative loss. The experimental data are combined to create an empirical summary of the effect of solid particles and correct the corresponding GIM input parameters. By comparing the prediction results with the experimental data, it can be seen that the CMDB propellant exhibits linear viscoelastic characteristics before the yield point. The loss tangent curve has a small secondary transition loss peak at low temperature and a large glass transition loss peak at high temperature. The values of Young's modulus and yield stress have obvious strain rate dependence, and both increase with an increase in the strain rate.

According to the constructed prediction method for the mechanical properties of the CMDB propellant, the influence of the NC/NG mass ratio in the binder on the mechanical properties of the CMDB propellant is analyzed over a wide strain rate range. With a decrease in the NC/NG mass ratio in the binder, the changes in the α and β transition temperatures are small, the peaks of the α and β loss peaks both increase, and the cumulative loss increases. At a certain strain rate, as the mass ratio decreases, Young's modulus and yield stress of the propellant increase. At a high strain rate, the change in the mass ratio has a greater effect on the increase in the Young's modulus. At the same time, the change in the mass ratio at each strain rate increases the yield stress. This law can provide a reference for the optimization design of CMDB propellant charge components.

In addition, when using the GIM method to establish the relationship between the propellant micromolecular structure and macromechanical properties, not only its structural characteristics but also the microstructure of the binder polymer may be affected by the manufacturing process. These uncertainty factors in the GIM input parameters have a certain influence and may lead to deviations in the prediction results.

In general, this study analyzes the influence of the binder matrix component mass ratio on the mechanical properties of propellants, which provides the possibility to judge whether the designed propellant can maintain structural integrity in the application environment by digital means rather than experimental means. The constitutive model under a wide strain rate considering the influence of particles proposed in this paper effectively makes up for the deficiency of CMDB propellants in the medium strain rate range and provides motivation and prospect for the research of propellant constitutive models in the wide strain rate range and the development of mechanical property prediction of particle-reinforced composites.

Nomenclature

σ_E: Engineering stress
ε_E: Engineering strain
$\dot{\varepsilon}$: Strain rate
σ: True stress
ε: True strain
T_g: Glass transition temperature
T_β: β transition temperature
tanδ: Loss tangent
α: Glass transition
β: β transition
r: The diameter of characteristic group unit
r_0: The value of r at absolute zero
L: The length of characteristic group unit
V: The volume of characteristic group unit
V_0: The value of V at absolute zero
V_W: van der Waals volume
E: The molecular group interaction energy
E_{coh}: The value of the potential function when $r = r_0$
N: Freedom of movement of the characteristic group

N_c: Number of degrees of freedom activated when the molecular chain is stretched
ΔN_β: The degree of freedom of the polymer
θ_1: Cooperative vibration reference temperature
C: Specific heat
R: Molar gas constant
α: Coefficient of thermal expansion
B_0: The pure elastic bulk modulus of the matrix
B: Pure elastic bulk modulus of the propellant
G_0: Pure elastic shear modulus of the matrix
T_{gr}: Glass transition temperature at 1 rad/s
f: Angular frequency
f_0: Reference angular frequency
$\tan \Delta_g$: α cumulative loss tangent
$\tan \Delta_\beta$: β cumulative loss tangent
$\tan \delta_g$: The distribution of the α loss tangent
$\tan \delta_\beta$: The distribution of the β loss tangent
s: Divergence of Gaussian distribution
ΔH_β: The activation energy of the β transformation
Y: Young's modulus
σ_y: Yield stress
ε_y: Yield strain
M: Molar mass of the characteristic group
m_i: Mass fraction of component i
n_i: Molecular weight of component i
V_i: Volume fraction of component i
DMA: Dynamic mechanical analysis
SHPB: Split Hopkinson pressure bar
CMDB: Composite modified double base
GIM: Group interaction model
NC: Nitrocellulose
NGN: Nitroglycerin
HTPB: Hydroxyl-terminated polybutadiene.

Data Availability

All data obtained or analyzed during this study are included in this published article.

Conflicts of Interest

The authors declare that they have no conflicts of interest.

References

[1] S. Chaoxiang, J. Xu, X. Chen, Z. Jian, Y. Zheng, and W. Wenqiang, "Strain rate and temperature dependence of the compressive behavior of a composite modified double-base propellant," *Mechanics of Materials*, vol. 89, pp. 35–46, 2015.

[2] C. Zhuo, F. Feng, and X. Wu, "Development process of muzzle flows including a gun-launched missile," *Chinese Journal of Aeronautics*, vol. 28, no. 2, pp. 385–393, 2015.

[3] L. Yang, N. Wang, K. Xie, X. Sui, and S. Li, "Influence of strain rate on the compressive yield stress of CMDB propellant at low, intermediate and high strain rates," *Polymer Testing*, vol. 51, pp. 49–57, 2016.

[4] C. R. Siviour, P. R. Laity, W. G. Proud et al., "High strain rate properties of a polymer-bonded sugar: their dependence on applied and internal constraints," *Proceedings of the Royal Society A: Mathematical, Physical and Engineering Sciences*, vol. 464, no. 2093, pp. 1229–1255, 2008.

[5] G. P. Sunny, *A high strain-rate investigation of a Zr-based bulk metallic glass and an HTPB polymer composite*, Doctoral dissertation, Case Western Reserve University, 2011.

[6] C. M. Cady, W. R. Blumenthal, G. T. Gray, and D. J. Idar, "Mechanical properties of plastic bonded explosive binder materials as a function of strain rate and temperature," *Polymer Engineering & Science*, vol. 46, no. 6, pp. 812–819, 2006.

[7] H. Zhang, H. Chang, X. Li, X. Wu, and Q. He, *The Effect of Strain Rate on Compressive Behavior and Failure Mechanism of CMDB Propellant*, Defence Technology, 2021.

[8] S. Y. Ho, "High strain-rate constitutive models for solid rocket propellants," *Journal of Propulsion and Power*, vol. 18, no. 5, pp. 1106–1111, 2002.

[9] C. X. Sun, Y. T. Ju, Y. Zheng, P. B. Wang, and J. F. Zhang, "Mechanical properties of double-base propellant at high strain rates and its damage-modified ZWT constitutive model," *Explosion and Shock Waves*, vol. 23, no. 1, pp. 16–22, 2013.

[10] Z. L. Liu, X. M. Wang, W. J. Yao, W. B. Li, and X. J. Liu, "Numerical simulation and mechanical behavior of base bleed grain at high strain rate," *Hanneng Cailiao/Chinese Journal of Energetic Materials*, vol. 22, no. 4, pp. 529–534, 2014.

[11] R. Kunz, "*Characterization of solid propellant for linear cumulative damage modelling*," in *45th AIAA/ASME/SAE/ASEE Joint Propulsion Conference & Exhibit*, Denver, Colorado, 2013.

[12] M. Burke, P. Woytowitz, and G. Reggi, *A nonlinear viscoelastic constitutive model for solid propellant*, 2013.

[13] H. C. Yildinm and S. Oezupek, "Structural assessment of a solid propellant rocket motor: effects of aging and damage," *Aerospace Science and Technology*, vol. 15, no. 8, pp. 635–641, 2011.

[14] Z. Wang, H. Qiang, T. Wang, G. Wang, and X. Hou, "A thermovisco-hyperelastic constitutive model of htpb propellant with damage at intermediate strain rates," *Mechanics of Time-Dependent Materials*, vol. 22, no. 3, pp. 291–314, 2018.

[15] J. K. Chen, Z. P. Huang, and Y. W. Mai, "Constitutive relation of particulate-reinforced viscoelastic composite materials with debonded microvoids," *Acta Materialia*, vol. 51, no. 12, pp. 3375–3384, 2003.

[16] J. K. Chen, Z. P. Huang, and M. Yuan, "A constitutive theory of particulate-reinforced viscoelastic materials with partially debonded microvoids," *Computational Materials Science*, vol. 41, no. 3, pp. 334–343, 2008.

[17] H. Tan, Y. Huang, and C. Liu, "The viscoelastic composite with interface debonding," *Composites Science and Technology*, vol. 68, no. 15-16, pp. 3145–3149, 2008.

[18] K. Tohgo, I. Yu, and Y. Shimamura, "A constitutive model of particulate-reinforced composites taking account of particle size effects and damage evolution," *Composites Part A Applied Science & Manufacturing*, vol. 41, no. 2, pp. 313–321, 2010.

[19] J. Hur, J. B. Park, G. D. Jung, and S. K. Youn, "Enhancements on a micromechanical constitutive model of solid propellant," *International Journal of Solids and Structures*, vol. 87, pp. 110–119, 2016.

[20] F. Xu, *Micromechanics approach to the study of constitutive response and fracture of solid propellant materials*, Dissertations & Theses - Gradworks, 2008.

[21] Y. Kohno, K. Ueda, and A. Imamura, "Molecular dynamics simulations of initial decomposition process on the unique N –N bond in nitramines in the crystalline state," *Journal of Physical Chemistry*, vol. 100, no. 12, pp. 4701–4712, 1996.

[22] M. R. Manaa, L. E. Fried, C. F. Melius, M. Elstner, and T. Frauenheim, "Decomposition of HMX at extreme conditions: a molecular dynamics simulation," *The Journal of Physical Chemistry A*, vol. 106, no. 39, pp. 9024–9029, 2002.

[23] J. Xiao, G. Fang, G. Ji, and H. Xiao, "Simulation investigations in the binding energy and mechanical properties of HMX-based polymer-bonded explosives," *Chinese Science Bulletin*, vol. 50, no. 1, pp. 21–26, 2004.

[24] D. Porter, *Group Interaction Modelling of Polymer Properties*, 1995.

[25] D. Porter and P. Gould, "Predictive nonlinear constitutive relations in polymers through loss history," *International Journal of Solids and Structures*, vol. 46, no. 9, pp. 1981–1993, 2009.

[26] J. Guan, Y. Wang, B. Mortimer et al., "Glass transitions in native silk fibres studied by dynamic mechanical thermal analysis," *Soft Matter*, vol. 12, no. 27, pp. 5926–5936, 2016.

[27] J. Jordan, D. Montaigne, P. Gould, C. Neel, G. Sunny, and C. Molek, "High strain rate and shock properties of hydroxyl-terminated polybutadiene (HTPB) with varying amounts of plasticizer," *Journal of Dynamic Behavior of Materials*, vol. 2, no. 1, pp. 91–100, 2016.

[28] J. Foreman, S. Behzadi, D. Porter, P. Curtis, and F. Jones, "Hierarchical modelling of a polymer matrix composite," *Journal of Materials Science*, vol. 43, no. 20, pp. 6642–6650, 2008.

[29] E. Davies and S. C. Hunter, "The dynamic compression testing of solids by the method of the split Hopkinson pressure bar," *Journal of the Mechanics and Physics of Solids*, vol. 11, no. 3, pp. 155–179, 1963.

[30] T. Murayama and C. Ford, *Dynamic Mechanical Analysis of Polymer Materials*, Elsevier, New York, 1988.

[31] R. C. Warren, "Transitions and relaxations in plasticised nitrocellulose," *Polymer*, vol. 29, no. 5, pp. 919–923, 1988.

[32] G. Weng, "Some elastic properties of reinforced solids, with special reference to isotropic ones containing spherical inclusions," *International Journal of Engineering Science*, vol. 22, no. 7, pp. 845–856, 1984.

[33] H. C. Dehm, *Composite modified double-base propellant with filler bonding agent*, 1977.

[34] Z. Zhou, Z. N. Jia, and Q. H. Zhou, "Research on dynamic mechanical properties of modified double base (CMDB) propellant," *Acta Armamentarii*, vol. 6, no. 2, pp. 49–58, 1985.

[35] V. Porter, F. Vollrath, and Z. Shao, "Predicting the mechanical properties of spider silk as a model nanostructured polymer," *European Physical Journal E Soft Matter*, vol. 16, no. 2, pp. 199–206, 2005.

[36] A. Bondi, "Physical properties of molecular crystals liquids, and glasses," *Journal of Molecular Structure*, vol. 19, no. 12, p. 429, 1968.

[37] N. Yao, Z. R. Liu, J. N. Wang, and L. Y. Zhang, "*Effect of RDX content on dynamic mechanical properties of modified double-base propellants*," *Journal of Propulsion Technology*, vol. 29, no. 4, pp. 498–501, 2008.